Int. J. Electrochem. Sci., 11 **(2016)** 2085 - 2096

International Journal of ELECTROCHEMICAL SCIENCE
www.electrochemsci.org

CNF-supported Platinum Electrocatalysts Synthesized Using Plasma-Assisted Sputtering in Pulse Conditions for the Application in a High-Temperature PEM Fuel Cell

Sergey A. Grigoriev[1,*], *Vladimir N. Fateev*[2], *Elena K. Lutikova*[2], *Alexander S. Grigoriev*[2], *Dmitri G. Bessarabov*[3], *Xing Wei*[4], *Junjie Ge*[4]

[1] National Research University "Moscow Power Engineering Institute", Krasnokazarmennaya str., 14, Moscow, 111250, Russia
[2] National Research Center "Kurchatov Institute", Kurchatov sq., 1, Moscow, 123182, Russia
[3] DST HySA Infrastructure Centre of Competence, Faculty of Engineering, North-West University, Potchefstroom, 2520, South Africa
[4] Changchun Institute of Applied Chemistry CAS, Renmin str., 5625, Changchun, 130002, China
[*]E-mail: sergey.grigoriev@outlook.com

Received: 2 December 2015 / *Accepted:* 20 January 2016 / *Published:* 1 February 2016

Nanostructured platinum catalysts for a high-temperature proton-exchange membrane (PEM) fuel cell based on polybenzimidazole (PBI) doped by H_3PO_4 were synthesized by magnetron-ion sputtering of platinum on carbon nano-fibers (CNF) in an impulse mode. The resulting catalysts were studied by transmission electron microscopy and X-ray diffraction. These catalysts with platinum particles size from 4 to 6 nm uniformly distributed over the CNF surface exhibit high efficiency. The electrodes based on the synthesized electrocatalysts were tested in a liquid electrolyte and as a component of PBI-based fuel cell. The fuel cell had power density *ca.* 300 mW/cm^2. Degradation tests showed that carbon carrier oxidation mainly determined the catalyst stability and stability of CNF was higher in comparison with Vulcan XC-72.

Keywords: PEM fuel cell; polybenzimidazole; electrocatalysis; magnetron-ion sputtering; carbon nano-fibers

1. INTRODUCTION

Proton-exchange membrane (PEM) fuel cells gained a considerable development over the past 50 years since invention of perfluorinated (Nafion®-type) polymer electrolyte. Such low-temperature (< 100°C) electrochemical devices are used for a number of mobile and stationary applications (*e.g.*

zero-emission transport, backup systems, portable electronics, aerospace sector, etc). Application of PEM fuel cells also start in power plants with electricity and heat co-generation.

For a number of applications fuel cell-based power plants have a reformer, which produces hydrogen-contain gas mixture from conventional fuels (natural gas, gasoline) or from methanol, ethanol, etc. [1, 2]. This hydrogen-contain gas mixture cannot be used directly in low-temperature H_2/O_2 PEM fuel cells because of relatively high concentration of impurities. Some of these impurities act as hydrogen diluents, and hence, reduce fuel cell efficiency [3, 4]. However, some admixtures are poisons for the Pt-based electrocatalysts used for fuel oxidation. For example, the reformate of natural gas obtained by water vapor conversion [3] mainly consists of H_2 (40-75 vol. %), CO_2 (20-25 vol. %), N_2 and H_2O (a few percent), and other compounds among which CO (0.5-2 vol. %) is the strongest poison for PEM fuel cell catalysts. The adverse effect of CO_2, N_2 and H_2O presence in the feed gas is mainly the dilution of the hydrogen [4] and some reduction of hydrogen partial pressure in the fuel. CO also dilute the hydrogen but (and this is the most negative effect) acts as a poison for the platinum-based electrocatalysts [6]. Thus the fuel cell efficiency can greatly decrease. It should be noted that CO_2 is not only an inert diluent whereas leads to the formation of CO by the reverse water-gas shift reaction. This reaction is catalyzed by platinum nano-particles [7] providing a decrease of fuel cell performances.

In order to reduce the CO contents, several methods such as sorption, catalytic oxidation and/or purification using a membrane separator can be applied [1, 2, 8, 9]. Such treatment allows reducing the concentration of CO in the fuel mixture below 0.005 vol. % (50 ppm) [10]. Some CO-tolerant electrocatalysts (*e.g.* with Ru addition) can be successfully used for hydrogen electro-oxidation at the fuel cell anode [11-12] at this low level of CO. However, the cost of the whole power plant with CO removal system is significantly increases.

The alternative strategy consists in increase of the fuel cell operating temperature in order to reduce the harmful influence of CO on platinum electrocatalysts. An increase of the PEM fuel cell operating temperature up to 180°C will increase the tolerance of anode platinum catalyst to CO up to 2-3 vol. % [13]. The operation at high temperature will also improve the kinetics of reactions, decrease of membrane resistance and allow reaching higher fuel cell efficiency. Additional improvement coming from possible engineering solutions: (i) the heat removing from the fuel cell stack can be utilized more efficiently and simply; (ii) a fuel cell, which operates at high temperature, can combine with a fossil fuel reformer more efficiently. Exhaust heat from operating fuel cells could be used for pre-heating of hydrocarbon fuel and/or water in the inlet of the reformer and in order to improve the energy efficiency of the system by providing an additional heat for the endothermic reactions of fossil fuel conversion [14].

Since Nafion® is stable only up to *ca.* 150°C [15], alternative membrane materials were developed for operation at temperatures up to 200°C. Among various alternative proton exchange membranes suitable for high-temperature fuel cell operation, the poly(2,21-(m-phenylene)-5,51-bibenzimidazole) doped by phosphoric acid (PBI/H_3PO_4) complex is one of the perspective candidates [16]. The interest of using PBI/H_3PO_4 membranes is associated with their low gas permeability, good chemical and thermal stability and sufficient flexibility at temperatures up to 230°C. An important difference between Nafion® and PBI/H_3PO_4 is that the conductivity of PBI/H_3PO_4 does not so strongly

depend on moisture since this is an acid-base complex. Thus, no external gas humidification is required for PEM fuel cell based on H_3PO_4-doped PBI membranes.

Carbon nano-fibers (CNF) are carbon filaments nanostructures in which the atoms of carbon are grouped in structures with diameters from several up to 100 nm and lengths up to 1000 μm [17, 18]. CNF has a graphitic nature and possess a three-dimensional typical structure. The textural edge of graphene planes provides suitable sites for the Pt impregnation that should potentially reduce migration and agglomeration of Pt nano-particles [19]. The interest of using CNF as an electrocatalyst carrier is also associated with their higher electric conductivity in comparison with Vulcan XC-72, which will facilitate the electron transfer occurring during electrochemical reactions and higher corrosion/oxidation resistance [20]. Moreover, nano-scale CNF materials with high aspect ratio form micro-porous structures with improved reactants/product transport properties and total electron conductivity in catalyst layer.

This paper is dedicated to the development and investigation of CNF-supported Pt catalysts for a high-temperature PBI/H_3PO_4-based PEM fuel cell and comparison of their performances with Vulcan-based catalysts.

2. EXPERIMENTAL SECTION

2.1. Membrane preparation

Raw poly[2,2'-(m-phenylene)-5,5'-bibenzimidazole] (figure 1) was synthesized and film on it basis with 30 μm thickness was cast according to the technique described elsewhere [21]. Obtained PBI film was doped by H_3PO_4 (up to 15M level) by boiling in the 85% acid solution at *ca.* 80°C for *ca.* 100 hours to obtain appropriate proton conductivity. In order to remove impurities contained in the PBI film the acid was changed several times during the doping process.

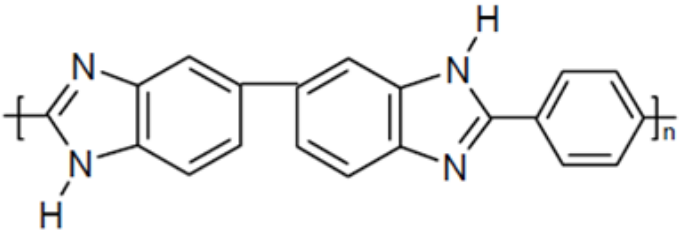

Figure 1. Chemical structure of PBI-chain.

2.2. CNF synthesis

CNF used as a support for Pt nano-particles were synthesized by a chemical vapor deposition (CVD) method [22] using planarGROW thermal CVD system (planarTECH LLC). C_2H_4/H_2 mixture with vol. ratio of 80/20 were catalytically decomposed at 500°C in the presence of unsupported NiO as catalyst precursor. The CNF growth time was 2 h.

In order to wash out the traces of catalyst used for CNF synthesis and to develop surface defects CNF were functionalized by treatment in H_2SO_4/HNO_3 (3/1). After decantation in deionized water CNT were additionally thermally treated at 350°C within 2 h. The surface defects serve as the metal condensation centers at magnetron-ion sputtering and if they are deficient, the metal atoms are preferably deposited on the already formed metal particles, but not on the free carbon surface. This leads to enlargement of metal particles and a decrease of the electrochemically active specific surface areas. Moreover, such functionalization allows to reduce Pt aggregation of Pt nano-particles during fuel cell operation.

2.3. Catalysts synthesis

Platinum nano-particles (40 wt. %) were deposited on CNF and Vulcan XC-72 using a laboratory DC magnetron sputtering system (figure 2) [23, 24] in an impulse mode. Magnetron sputtering was carried out in Ar atmosphere at discharge power 70 W.

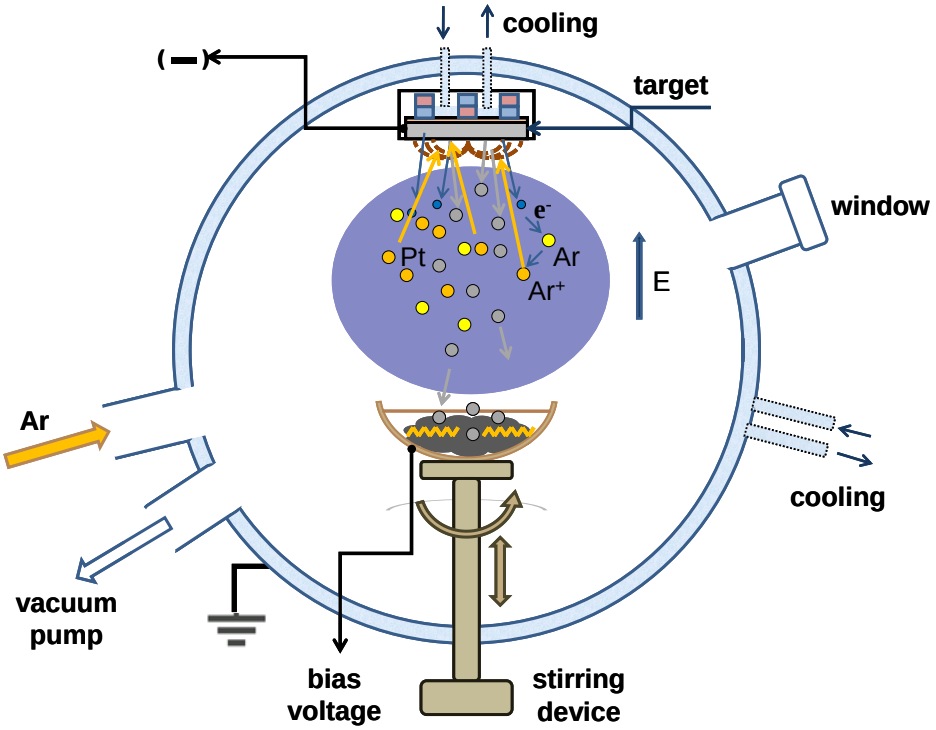

Figure 2. Schematic diagram of the magnetron sputtering unit.

Periodically (each 20 seconds) cathode potential (-100 V) was applied to the cup with carrier to provide Pt atoms acceleration and additional catalyst surface treatment with Ar ions. Such a treatment improved Pt particles adhesion to the surface and increased electrochemical active surface area. The carrier was placed as a layer with a thickness of *ca.* 2 mm on the bottom of the cup; the diameter of the cup was 115 mm; the height of the wall 25 mm; the distance between the target being sprayed and the powder surface 65 mm. The bias voltage was applied to a ring with two crossed spirals that touched the bottom of the cup. The spirals also provided the stirring of the powder when the cup was rotated.

The cup vibration frequency was 2-3 Hz; the vibration amplitude was *ca.* 1 mm; the cup rotation rate was *ca.* 10 rpm. The pumping-out was organized up to the pressure in the chamber of 6.7×10^{-3} Pa. Then, the working gas (Ar) was injected up to the pressure of 0.4 Pa.

Pt black and Pt40/Vulcan XC-72 were also synthesized using chemical methods described in details elsewhere [25, 26] and used for comparison.

2.4. CNF and catalysts characterization

Morphology of the synthesized materials was investigated by using a scanning electron microscope (SEM) Helios NanoLab 600i (FEI, US) attached with energy dispersive X-ray (EDX) spectrometer (EDAX, Mahwah, NJ, US). All SEM images were obtained in secondary electrons (SE) detection mode.

After that the specimens were studied in a transmission/scanning electron microscope (TEM/STEM) Titan 80-300 (FEI, Oregon, US) which have a spherical aberration corrector, a high angle annular dark field (HAADF) (Fischione, US) detector, EDX spectrometer (EDAX, Mahwah, NJ, US) and Gatan Image Filter (GIF; Gatan, Pleasanton, CA, US) after column. The TEM analyses were performed at 300 kV. This study provides the information on Pt nano-particles and CNF with atomic resolution.

Samples for TEM analysis were obtained by ultrasonic treatment of catalyst in ethanol for 10 minutes and deposition of the solution on standard Cu grid covered with Lacey© carbon film.

The cyclic voltammograms (CVs) were measured in Ar-saturated 1M H_2SO_4 at 25°C in a three-electrode glass cell. The measurements were performed using Solartron 1285 (Solarton Analytical) potentiostat. A saturated Ag/AgCl/KCl electrode (SSCE) were used as the reference electrode and a Pt wire were used as a counter electrode. A glassy carbon disk electrode with a surface area of 0.4 cm^2 with a catalytic layer deposited on it serve as a working electrode. The potential was applied in the range from -0.17 to 1.2 V *vs.* SSCE at a scan rate of 20 mV/s.

2.5. MEA preparation

MEA with the geometrical area of 7 cm^2 was fabricated using Sigracet® GDL 38 BC (SGL Carbon GmbH) carbon-fiber paper (disks of 30 mm in diameter, *ca.* 0.3 mm thick, and *ca.* 80% effective porosity) as gas diffusion layers (GDL) on cathode and anode. The catalytic inks for anode and cathode contain 0.4 mg/cm^2 of Pt black, or Pt supported on Vulcan XC-72 or CNF (40 wt % of Pt). This inks have been ultra-sonicated in 2-propanol and have been sprayed over the surface of GDLs.

2.6. Cell description and test conditions

A lay-out of the electrochemical cell used to measure polarization curves is shown on figure 3. The cell consists of two titanium end-plates with graphite-based flow-field plates [27] clamping down the membrane-electrode assembly with pressure of 50 kg/cm^2. Carbonaceous rings of polymer (Viton®) were used as cell sealants.

Electrolytic grade hydrogen and oxygen were used as fuel and oxidant in the fuel cell. A high-temperature circulation thermostat with a polymethylsiloxane-based heat transfer agent has been used to manage the fuel cell temperature. Before operation, the fuel cell was kept at 180°C for 30 minutes in order to facilitate the bounding of electrodes with membrane. Current-voltage performances have been recorded at 2 bars gas pressures and cell temperature of 180°C.

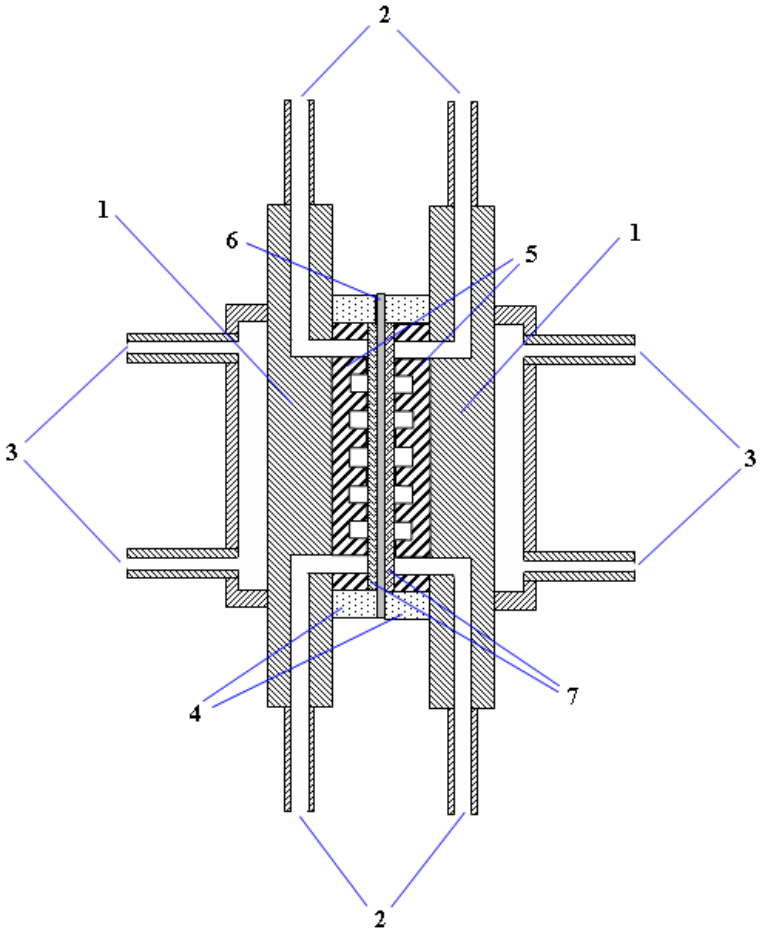

Figure 3. Lay-out of the laboratory PEM fuel cell.
1 – titanium half-cell; 2 – connecting pipes for reactant/product feeding/remove; 3 – connecting pipes for heating/cooling; 4 – sealants; 5 – graphite-based flow-field plates; 6 – PBI/H_3PO_4-based membrane; 7 – GDLs with electrocatalytic layers.

In order to accelerate degradation processes each MEA was exposed to repeated 300 on/off cycles (each 1 hour).

2.7. Accelerated degradation and oxidation experiments with Pt/CNF and Pt/Vulcan XC-72

For accelerated degradation and oxidation experiments we used frequently repeated fuel cell turn on/turn off cycles at 190°C at 4 bars gas pressure. "Turned on/turned off" repeating cycles were: the cell was operating 30 min at 800 mV; turned off for 5 min; operating 30 min at 600 mV; turned off for 5 min. Preliminary tests demonstrated that use of such turn on/turn off cycles resulted in a much

faster degradation of fuel cell electrochemical parameters in comparison with a stationary operation modes (probably due relatively quick changes of catalyst and carrier surface composition). Increased pressure and temperature assisted the degradation process.

Losses of catalysts weight during their oxidation in air at 200-500°C were also measured for accelerated tests of their stability using TA Instruments SDT2960 derivatograph. 350°C was chosen as the main test temperature to reduce the testing time and to increase the reproducibility.

3. RESULTS AND DISCUSSION

3.1. Structural parameters of CNF and catalysts

SE SEM image of CNF is presented in figure 4. The CNF represents the aggregation of fibers 0.1-0.2 μm in diameter. The ends of the fibers were not visible on the micrographs and that did not allow to estimate the fibers length.

The bright field (BF) STEM image of Pt/CNF catalysts is presented in figure 5(a). The enlarged BF STEM image of a fiber with Pt nano-particles is presented in figure 5(b), revealed that mostly they exhibit equiaxed morphology. According to BF STEM images, the samples synthesized using magnetron-ion sputtering in an impulse mode exhibit platinum particles size from 4 to 6 nm uniformly distributed over the CNF surface. STEM data for Pt/Vulcan XC-72 obtained by magnetron sputtering and chemical reduction were rather similar (see also [20]).

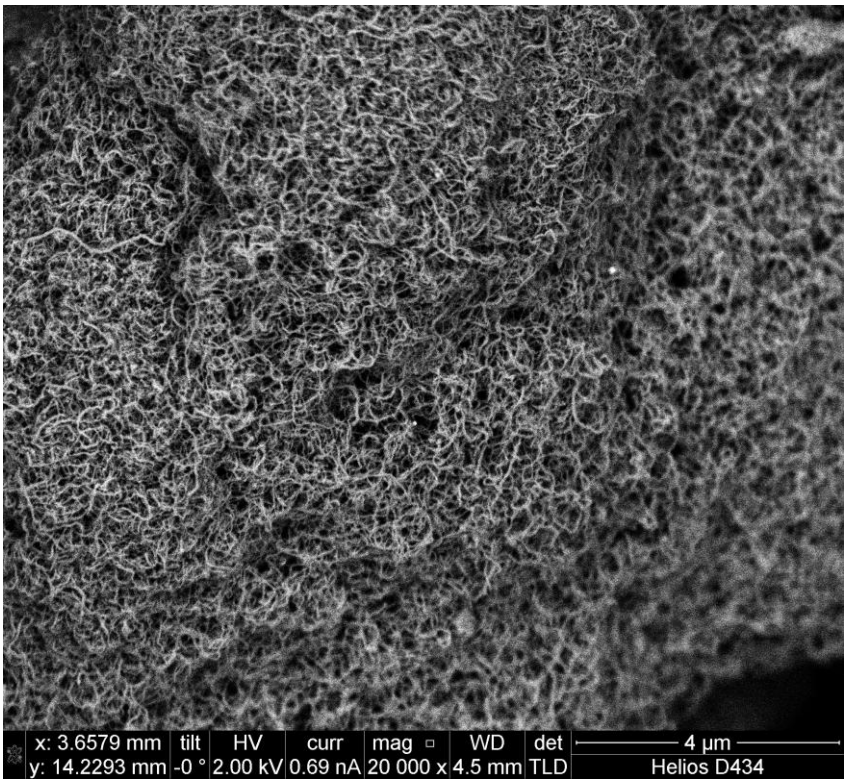

Figure 4. SE SEM image of CNF.

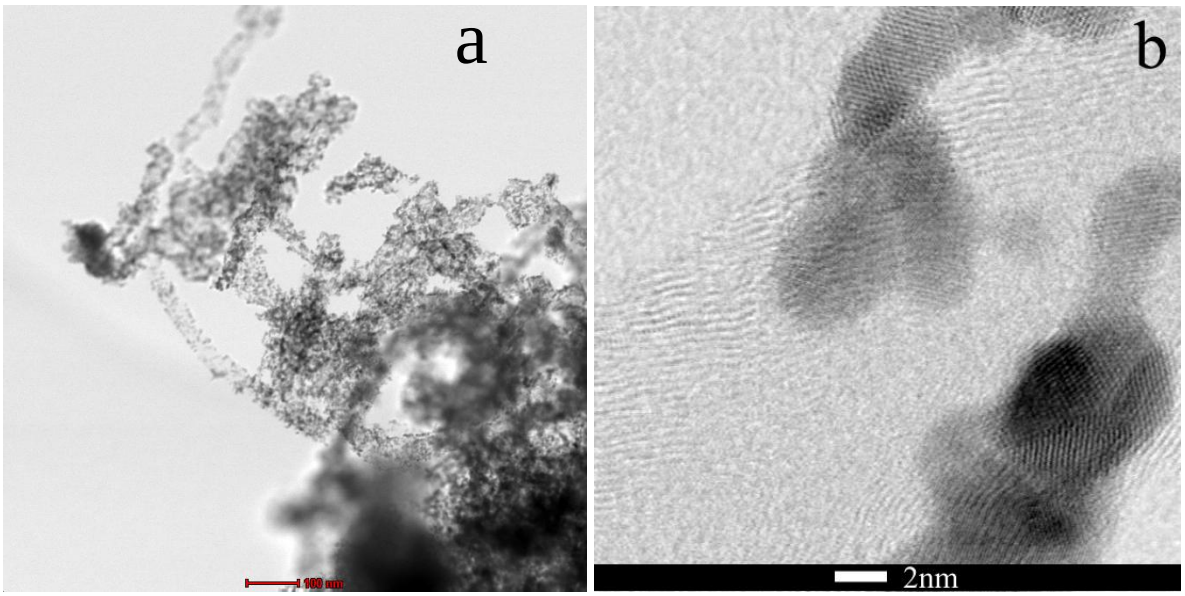

Figure 5. STEM images of Pt/CNF catalysts.

The EDX spectra (figure 6) unambiguously indicated that the system consisted of Pt and C without any impurities. Cu peaks have come from the copper grid used as support for the sample.

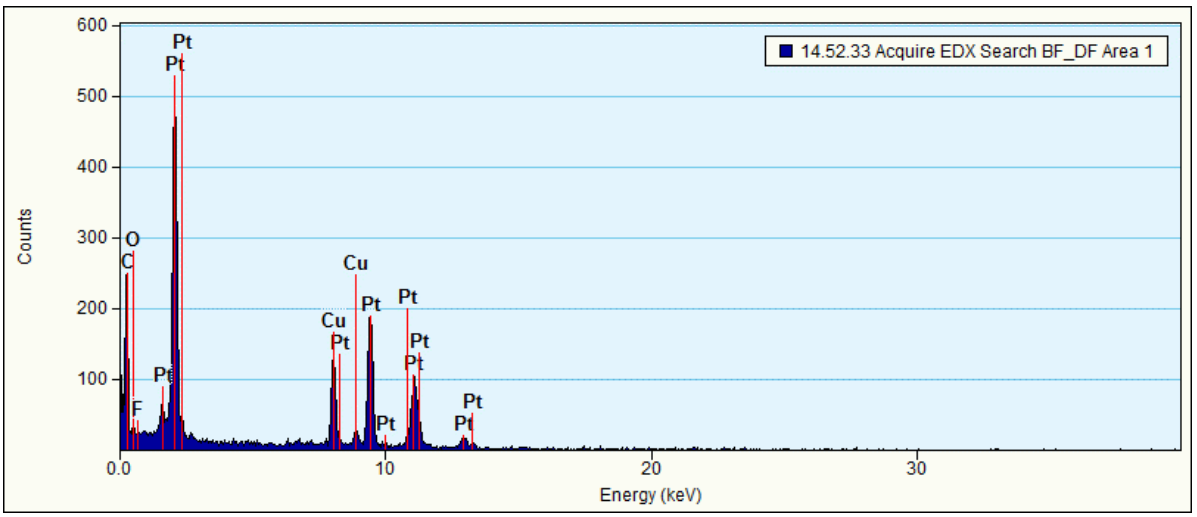

Figure 6. Energy-dispersive spectra of Pt/CNF catalysts.

Figure 7 shows CVs measured for Pt black, Pt/CNF and Pt/Vulcan XC-72 electrodes, voltage is specified *vs.* normal hydrogen electrode (NHE). In case of CNF and Vulcan XC-72 without Pt there were no any peaks on CV curves and currents were *ca.* 10 times less at potential less than 0.5 V and *ca.* 4 times less at potentials more than 0.5 V. So CV curves for catalysts characterize mainly Pt nanoparticles.

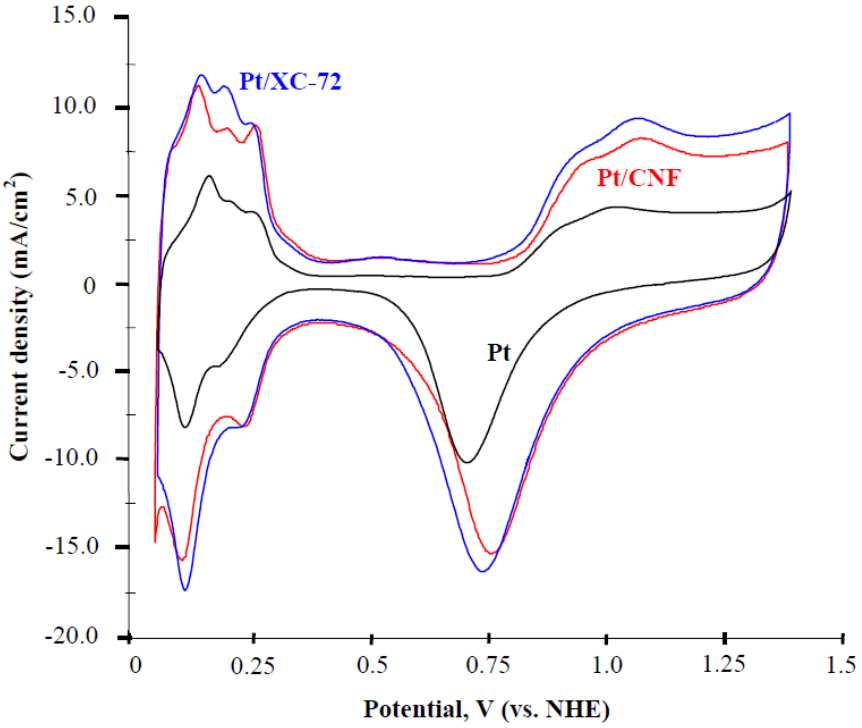

Figure 7. CV curves for Pt, Pt/Vulcan XC-72 and Pt/CNF-based electrodes (scan rate 20 mV/s).

One can see from figure 7 that CV curves for each catalysts have clear peaks and shapes appropriate for Pt (distinct peaks of hydrogen sorption-desorption in potential region 0.04-0.4 V, Pt surface oxidation at 0.8-1.25 V and reduction of Pt surface oxides at 1.0-0.5 V). Some small difference in a shape of CV curves in hydrogen region (0.04-0.4 V) for Pt/Vulcan XC-72 and Pt/CNF-based electrodes could be attributed to some difference in platinum particles surface structure (domination of different crystal faces on the surface) and/or difference in Pt-carbon interaction. But at first approximation the electrochemical active surface area of such catalysts (table 1) could be evaluated by the integration of hydrogen desorption peaks on the CV curve using the technique described in detail in [25].

Table 1. Electrochemical active surface areas of synthesized electrocatalysts.

Electrocatalysts	**Electrochemical active surface area, m^2/g**
Pt40/Vulcan XC-72	62
Pt40/CNF	57
Pt	34

3.2. Tests in the cell

The current-voltage performances were measured at 180°C and 2 bars before and after stability, tests (see figure 8).

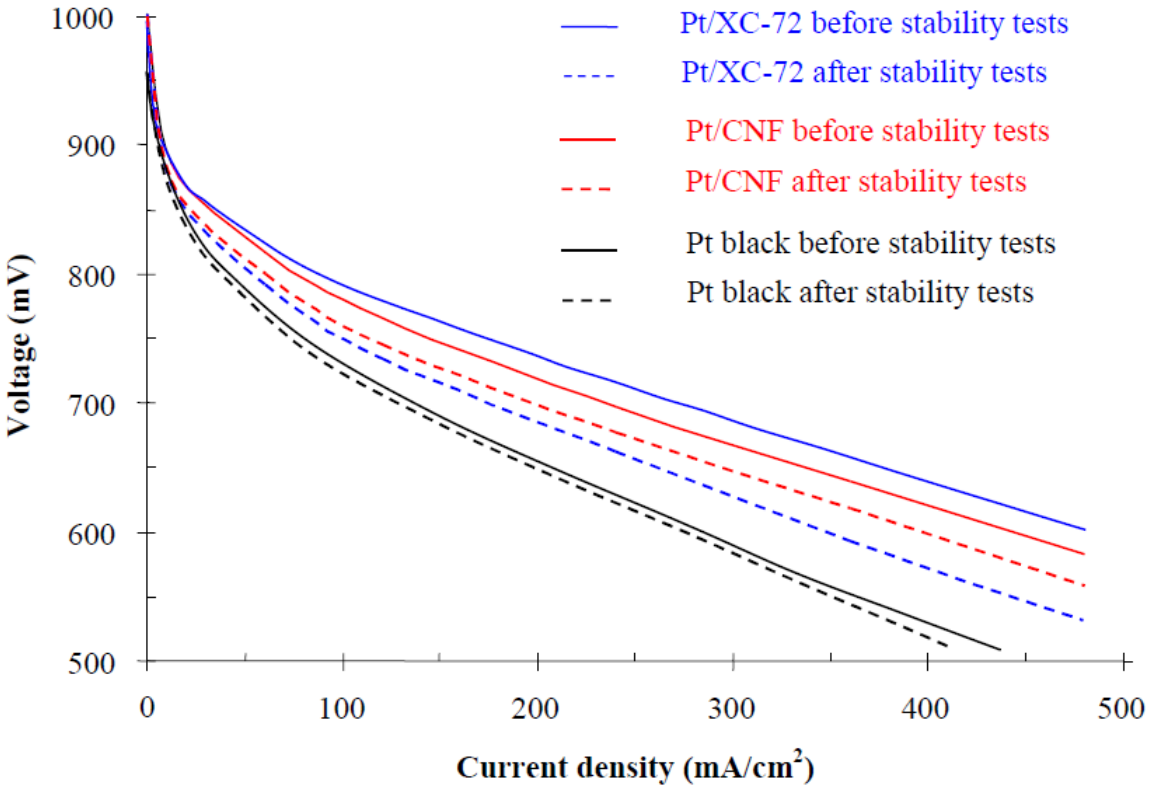

Figure 8. Current-voltage curves of MEAs based on Pt, Pt/Vulcan XC-72 and Pt/CNF before and after stability tests (300 on/off cycles) in H_2-O_2 operation mode.

Initial current-voltage curves are consistent with those reported by other research groups and our own results [13, 21]. In particular, a cell had a power density *ca.* 300 mW/cm^2 both for Pt40/Vulcan XC-72 and Pt40/CNF at 0.5-0.6 V. During degradation tests using turn on/turn off cycles we observed a rather monotonous currents decrease with time at fixed voltages. Pt black electrocatalyst had lower activity but demonstrated significantly higher stability than Pt catalysts supported on carbon carriers. Hence, one can suppose that fuel cell degradation takes place mainly because of the corrosion (oxidation) of carbon carrier.

Making the comparison of current-voltage curves plotted on figure 8 it is possible to conclude that Pt/Vulcan XC-72 initially demonstrates better performances in comparison with Pt/CNF (because of the electrochemical active surface area difference). However, after stability tests the degradation of Pt/Vulcan XC-72 is higher; Pt/CNF does not exhibit significant losses of performances after stability tests.

Experiments with Pt/Vulcan XC-72 and Pt/CNF oxidation in air at 350°C demonstrate higher stability of Pt/CNF as well. Weight losses of Pt/CNF were 6-10 wt. % only while Pt/Vulcan XC-72 weight losses reached 45-50%.

4. CONCLUSIONS

Developed method of plasma-assisted magnetron sputtering in an impulse mode has shown promising potentialities for the synthesis of high-quality carbon-supported platinum electrocatalysts. Synthesized CNF-based Pt catalyst demonstrates excellent structural and electrochemical properties and good performances in a high-temperature PEM fuel cell with H_3PO_4-doped PBI membrane. In particular, an output cell power was *ca.* 300 mW/cm^2.

Degradation tests have shown that the corrosion of carbon carrier is an important issue as it effects on the lifetime and durability of the catalyst. Carbon black (Vulcan XC-72) is the most widely used catalyst support, but it corrosion occurs during PEM fuel cell operation, and is accelerated at high-temperatures and on/off cycles. It was shown that in high-temperature PEM fuel cell Pt/CNF is more stable in comparison with Pt/Vulcan XC-72.

ACKNOWLEDGEMENTS
Development of pulse magnetron sputtering method of electrocatalyst synthesis, catalysts preparation and CVs measurements were executed with financial support of the Russian Science Foundation (project No. 14-29-00111). Synthesis and investigation of carbon nano-fibers was supported by the Russian Foundation for Basic Research within the framework of research project No. 14-29-04071 ofi_m. Fuel cell tests were financially supported by the Ministry of Education and Science of the Russian Federation within the framework of government task No. 2014/123 (amendment no 1) for performance of the government works in scientific activities. Authors acknowledge Dr. M.Yu. Presnyakov (Kurchatov Institute) for his help with the characterization of the catalysts.

References

1. J. Mathiak, A. Heinzel, J. Roes, Th. Kalk, H. Kraus, H. Brandt, *J Power Sources*, 131 (2004) 112.
2. A. Lotrič, M. Sekavčnik, S. Hočevar, *J Power Sources*, 270 (2014) 166.
3. S.A. Grigor'ev, V.N. Fateev, V.G. Sister, V.D. Rusanov, *Doklady Physical Chemistry*, 2006 (411) 293.
4. S. Grigoriev, L. Madier, S. Martemianov, N. Drozdova, Summaries of the 17th International Congress of Chemical and Process Engineering CHISA 2006 (Prague, Czech Republic, 27-31 August 2006), Vol. 1, pp. 244-245.
5. C. Song, *Catalysis Today*, 77 (2002) 17.
6. R.J. Bellows, E.P. Marucchi-Soos, D.T. Buckley, *Ind. Eng. Chem. Res.*, 35 (1996) 1235.
7. A.-K. Meland, S. Kjelstrup, *Journal of Electroanalytical Chemistry*, 610 (2007) 171.
8. P. Millet, R. Ngameni, C. Decaux, S.A. Grigoriev, *Int J Hydrogen Energ*, 36 (2011) 4262.
9. C. Decaux, R. Ngameni, A. Ranjbari, S. Grigoriev, P. Millet, *Int J Hydrogen Energ*, 38 (2013) 8584.
10. P. Costamagna, S. Srinivasan, *J Power Sources*, 102 (2001) 242.

11. L. Zhang, J. Kim, J. Zhang, F. Nan, N. Gauquelin, G.A. Botton, P. He, R. Bashyam, S. Knights, *Applied Energy*, 103 (2013) 507.
12. T.R. Ralph, M.P. Hogarth, *Platinum Metals Rev.*, 46 (2002) 117.
13. K. Kwon, D.Y. Yoo, J.O. Park, *J Power Sources*, 185 (2008) 202.
14. F. Weng, C.-K. Cheng, K.-C. Chen, *Int J Hydrogen Energ*, 38 (2013) 6059.
15. C. Fiori, A. Dell'Era, F. Zuccari, A. Santiangeli, A. D'Orazio, F. Orecchini, *Int J Hydrogen Energ*, 40 (2015) 11949.
16. A.Y. Leykin, A.I. Fomenkov, E.G. Galpern, I.V. Stankevich, A.L. Rusanov, *Polymer*, 51 (2010) 4053.
17. K.P. de Jong, J.W. Geus, *Catalysis Reviews - Science & Engineering*, 42 (2000) 481.
18. P. Trogadas, T.F. Fuller, P. Strasser, *Carbon*, 75 (2014) 5.
19. I. Kvande, N. Hammer, M. Rønning, D. Chen, S.T. Briskeby, M. Tsypkin, S. Sunde, R. Tunold, *Topics in Catalysis*, 45 (2007) 81.
20. M.S. Mamat, S.A. Grigoriev, K.A. Dzhus, G.S. Walker, D.M. Grant, *Int J Hydrogen Energ*, 35 (2010) 7580.
21. S.A. Grigoriev, N.V. Kuleshov, A.S. Grigoriev, P. Millet, *Journal of Fuel Cell Science and Technology*, 12 (2015) 031004.
22. S.A. Grigoriev, M.S. Mamat, K.A. Dzhus, G.S. Walker, P. Millet, *Int J Hydrogen Energ*, 36 (2011) 4143.
23. A.A. Fedotov, S.A. Grigoriev, P. Millet, V.N. Fateev, *Int J Hydrogen Energ*, 38 (2013) 8568.
24. S.A. Grigoriev, A.A. Fedotov, S.A. Martemianov, V.N. Fateev, *Russian Journal of Electrochemistry*, 50 (2014) 638.
25. S.A. Grigoriev, P. Millet, V.N. Fateev, *J Power Sources*, 177 (2008) 281.
26. S.A. Grigoriev, P. Millet, K.A. Dzhus, H. Middleton, T.O. Saetre, V.N. Fateev, *Int J Hydrogen Energ*, 35 (2010) 5070.
27. S.A. Grigoriev, A.A. Kalinnikov, N.V. Kuleshov, P. Millet, *Int J Hydrogen Energ*, 38 (2013) 8557.

© 2016 The Authors. Published by ESG (www.electrochemsci.org). This article is an open access article distributed under the terms and conditions of the Creative Commons Attribution license (http://creativecommons.org/licenses/by/4.0/).